# Discovery of knock-down resistance in the major African malaria vector *Anopheles funestus*.

**Authors**

Joel O. Odero[1,2*] ✉, Tristan P. W. Dennis[3*], Brian Polo[4], Joachim Nwezeobi[5], Marilou Boddé[5], Sanjay C. Nagi[3], Anastasia Hernandez-Koutoucheva[5], Ismail H. Nambunga[1], Hamis Bwanary[1], Gustav Mkandawile[1], Nicodem J Govella[1], Emmanuel W. Kaindoa[1], Heather M. Ferguson[2], Eric Ochomo[4], Chris S. Clarkson[5], Alistair Miles[5], Mara K. N. Lawniczak[5], David Weetman[3#], Francesco Baldini[1,2#], Fredros O. Okumu [1,2#]✉

[*]These authors contributed equally to this work

#These authors equally supervised this work

✉ Corresponding author

**Affiliations**

1. Environmental Health and Ecological Sciences Department, Ifakara Health Institute, Ifakara, Tanzania
2. School of Biodiversity, One Health, and Veterinary Medicine, G12 8QQ, University of Glasgow, Glasgow, UK
3. Department of Vector Biology, Liverpool School of Tropical Medicine, L3 5QA, Liverpool, UK
4. Entomology Section, Centre for Global Health Research, Kenya Medical Research Institute, Kisumu, Kenya
5. Wellcome Sanger Institute, Wellcome Genome Campus, Hinxton, CB10 1SA, UK.

## Abstract

A major mechanism of insecticide resistance in insect pests is knock-down resistance (*kdr*) caused by mutations in the voltage-gated sodium channel (*Vgsc*) gene. Despite being common in most malaria *Anopheles* vector species, *kdr* mutations have never been observed in *Anopheles funestus*, the principal malaria vector in Eastern and Southern Africa. While monitoring 10 populations of *An. funestus* in Tanzania, we unexpectedly found resistance to DDT, a banned insecticide, in one location. Through whole-genome sequencing of 333 *An. funestus* samples from these populations, we found 8 novel amino acid substitutions in the *Vgsc* gene, including the *kdr* variant, L976F (L1014F in *An. gambiae*), in tight linkage disequilibrium with another (P1842S). The mutants were found only at high frequency in one region, with a significant decline between 2017 and 2023. Notably, *kdr* L976F was strongly associated with survivorship to the exposure to DDT insecticide, while no clear association was noted with a pyrethroid insecticide (deltamethrin). Further study is necessary to identify the origin and spread of *kdr* in *An. funestus*, and the potential threat to current insecticide-based vector control in Africa.

## Significance

Knock-down resistance (kdr) mutations confer resistance to malaria vector control insecticides and pose a grave threat to malaria control. Here, we report the first discovery of kdr in *An. funestus*, the principal malaria vector in East and Southern Africa. Kdr in *An. funestus* conferred resistance to DDT but not deltamethrin. Based on extensive DDT contamination and unofficial usage in Tanzania, it is possible that kdr emerged because of widespread organic pollution as opposed to through public health efforts. Regardless of origin, the discovery of kdr in *An. funestus* is an alarming development that warrants immediate, extensive follow-up and close surveillance to establish the origin, and extent to which it may threaten malaria control in *An. funestus*.

52 **Introduction**

53 Chemical insecticides are central to the control of agricultural pests and
54 disease vectors. The control of *Anopheles* mosquitoes through the distribution of over
55 2.9 billion insecticide-treated bed nets (ITNs) has helped avert an estimated 633
56 million cases of malaria (*1*) - a disease that still kills 600,000 yearly (*2*). However, the
57 widespread use of insecticides for agricultural pest and disease vector control also
58 has detrimental consequences, including direct lethal and sub-lethal effects on
59 human and animal health (*3, 4*) and destabilizing effects on ecosystem structure and
60 function. For example, insecticide exposure is a key stressor affecting the population
61 decline of pollinators, essential for ecosystem health and food production (*5, 6*).

62 A key obstacle to the sustainable control of malaria is the evolutionary arms
63 race between mosquitoes and insecticide-based mosquito control. Strong selection
64 pressures generated by insecticide-based agricultural pest and disease vector control
65 activities have resulted in the independent evolution of a diverse range of
66 mechanisms that confer insecticide resistance (IR) phenotypes in numerous insect
67 species (*7*). One of the earliest described IR mechanisms was the emergence of
68 knock-down resistance (*kdr*), mediated by mutations in the target site of pyrethroid
69 and organochlorine insecticides, located in the voltage-gated sodium channel gene
70 (*Vgsc*), an essential component of the nervous system (*8*). These *kdr*-driven resistance
71 phenotypes appeared rapidly after the introduction of the organochlorine dichloro-
72 diphenyl-trichloroethane (DDT) spraying for insect control in the mid-20th century
73 (*9*) and eventually evolving to confer resistance to pyrethroids (*10, 11*), the key
74 ingredient in ITNs - the first line of defence against malaria. In an era of stalling
75 gains in malaria control (*2*), and concerted efforts both to develop a new generation
76 of ITN and IRS products (*12, 13*) and proactively manage the deployment of existing
77 insecticides to maximise efficacy, intensified surveillance, including genomic
78 surveillance (*14, 15*), of malaria vector populations is critical for providing real-time
79 warning of insecticide resistance emergence.

80 As part of phenotypic and genomic surveillance done in Tanzania to
81 understand the evolution and spread of insecticide resistance in *Anopheles funestus* -
82 the dominant malaria vector in Eastern and Southern Africa (*16*), we report the first
83 discovery of *kdr* mutations in *An. funestus.* We discover that this mutation confers
84 resistance to DDT, but not deltamethrin, despite a complete ban on DDT use for
85 agriculture and vector control in Tanzania since 2008 (*17*). We suggest
86 environmental contamination from extensive DDT stockpiles (*18*), or unofficial
87 agricultural use, as possible causes. The emergence of *kdr*, which threatens the
88 control of major crop pests and vectors of disease, such as *An. gambiae* and *Aedes*
89 *aegypti* (*19*), highlights the potential of chemical insecticide contamination or
90 unofficial use to exert unexpected and potentially harmful impacts on public health.

91 **Results**

92 Resistance to all major classes of insecticide is common in *An. funestus* and is
93 primarily mediated through the increased activity of enzymes that bind to and
94 metabolise insecticides (metabolic resistance) (*20, 21*). This contrasts with another
95 major vector *An. gambiae* where resistance is mostly conferred by a combination of
96 metabolic and target-site resistance (*7*). As part of an insecticide resistance
97 surveillance study in 10 sites across Tanzania (**Fig. 1A**) (*22*), we investigated
98 phenotypic resistance (as measured by mosquito survival 24 hours following
99 insecticide exposure) in *An. funestus* to the discriminating doses of DDT,
100 deltamethrin (type II pyrethroid), or deltamethrin together with the piperonyl
101 butoxide (PBO) synergist, which is increasingly used on ITNs (*23*) to restore
102 susceptibility in pyrethroid-resistant populations in Tanzania. The mosquitoes were
103 phenotypically resistant to deltamethrin in all regions, but PBO ubiquitously
104 restored susceptibility. Unexpectedly, resistance to DDT was recorded in the
105 Morogoro region (68%, CI 57.8 - 77.9), but not in other regions (**Fig. 1B**).

106 To understand the genetic bases of resistance, we analysed whole-genome-
107 sequencing (WGS) data from 333 mosquitoes sampled from 10 sites across Tanzania

108 (**Fig. 1A**). We performed genome-wide selection scans (GWSS) with the G123
109 statistic to test for evidence of selective sweeps in the *An. funestus* genome associated
110 with known or novel IR loci (**Fig. 1C**; grouping samples by administrative region
111 (see **Supp. Table 1** for per-group sample numbers). We detected a clear signal of
112 elevated G123 in the region containing the *Vgsc* gene in samples from the Morogoro
113 region in the southeastern part of the country (**Fig. 1C**). Notably, *Vgsc* encodes for
114 the voltage-gated sodium channel, where DDT binds in mosquitoes, and where
115 mutations are strongly linked to resistance in *An. gambiae* (*11*). In Kagera, Katavi, and
116 Mwanza regions, there was no visible sign of a selective sweep at or near the *Vgsc*
117 region. In Dodoma, Lindi, Ruvuma, and Tanga, there were peaks of elevated G123
118 near to *Vgsc*, but these appeared within the context of relatively high G123 across the
119 chromosome **(Fig. 1C).**

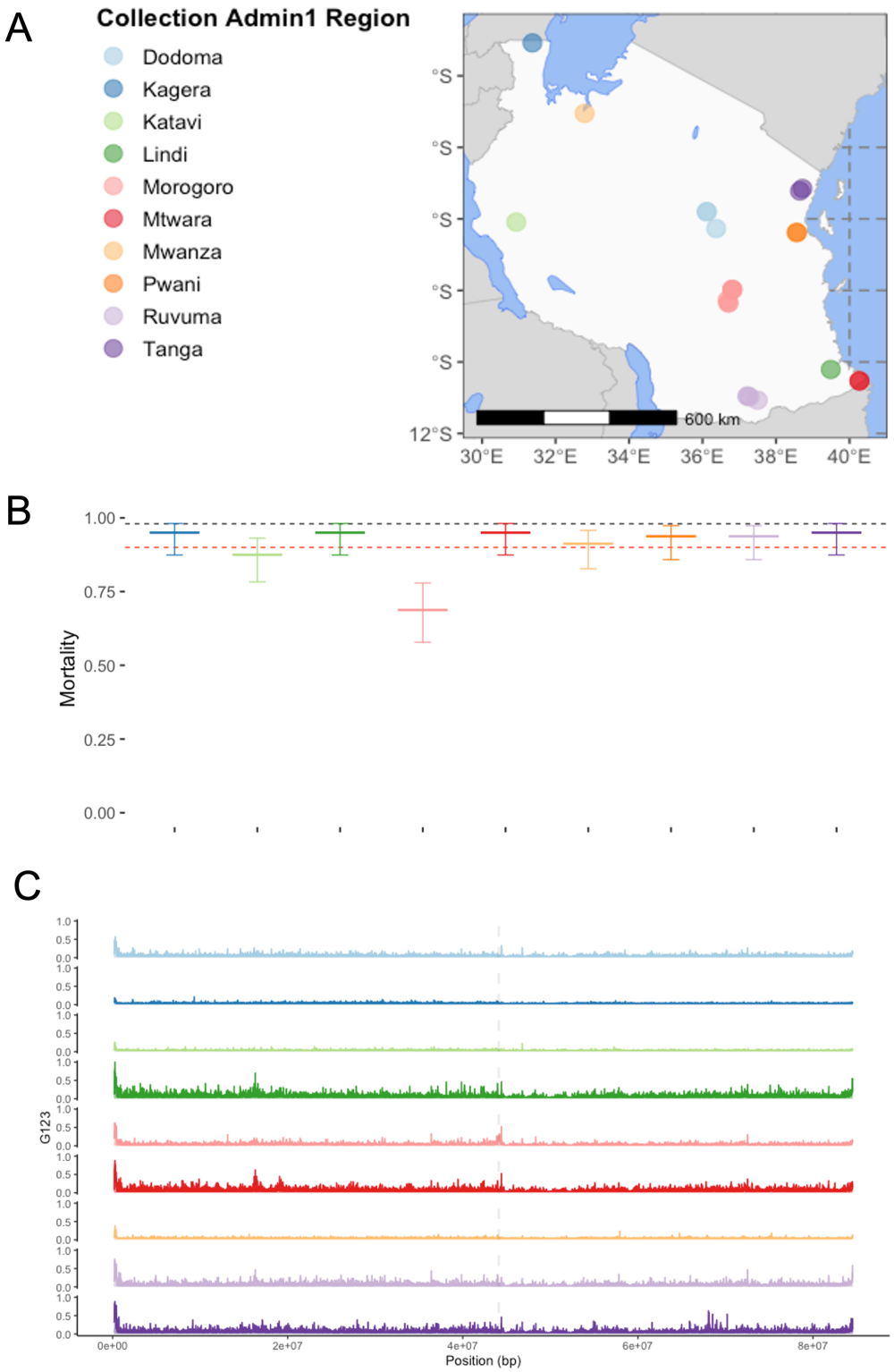
A
Collection Admin1 Region
Dodoma
Kagera
Katavi
Lindi
Morogoro
Mtwara
Mwanza
Pwani
Ruvuma
Tanga
°S
°S
°S
°S
°S
12°S
600 km
30°E
32°E
34°E
36°E
38°E
40°E
B
1.00
0.75
0.50
0.25
0.00
Mortality
C
G123
0e+00
2e+07
4e+07
6e+07
8e+07
Position (bp)

**Fig. 1: (A)** Map of *An. funestus* collection locations. Points indicate sample collection locations. The point colour indicates the administrative region from which samples were collected. **(B)**: Phenotypic insecticide resistance profile of *An. funestus* to DDT using bioassay data adopted from our recent surveillance (*22*). The colours represent the various regions where the bioassays were conducted, and the error bars are 95% confidence interval. The black and red dotted lines on the y-axis represent the 98 and 90% mortality thresholds. (**C**) G123 selection scans of *An. funestus* chromosome 3RL, coloured and windowed by sample collection region (where n>20 – see **Supp Table 2**). X-axis indicates the position (in base-pairs (bp)), Y-axis indicates the selection statistic G123. The Grey dotted line indicates the location of the *Vgsc* gene. Note Mwanza region is absent from panel **C** as there were too few samples (n<20) to perform a selection scan.

Mutations in *Vgsc* confer *kdr* in numerous pest and insect taxa (*24*). While not previously reported in *An. funestus*(*25*), *kdr* mutations in major malaria vectors within the *An. gambiae* complex are subject to intense selection (*26, 27*) and confer resistance to pyrethroid and organochlorine insecticides used in ITNs and insecticide sprays (*11, 24*). We searched our data for mutations in the *Vgsc* gene and found 8 amino acid substitutions occurring at frequencies greater than 5% (**Fig. 2A**). Of these, two alleles, L976F and P1842S occurred at the highest frequency (**Fig. 2A**). The frequencies of P1824S and L976F were highest in samples collected from Morogoro in 2017 (0.75 and 0.90 respectively) **(Fig. 2A)** and declined yearly, reaching their lowest frequency in samples collected in 2023 (0.48 and 0.56 respectively; $\chi^2 = 12.15$, p=0.0005; **Fig. 2B).** These mutations occurred at very low frequencies or were absent in all other locations (**Fig. 2A).** To understand their function, we aligned the *An. funestus Vgsc* sequence (Gene ID: AFUN2_008728.R15290) with that of *Musca domestica* (Gene ID: X96668) and *An. gambiae* (AGAP004707-RD AgamP4.12 gene set) (*27*). We found that the amino acid change at *An. funestus* L976F corresponded to L1014F in *M. domestica* and L995F in *An. gambiae* in domain II subunit 6 (IIS6) of the *Vgsc* gene (**Table 1**), which in *An. gambiae* species complex drastically increases IR to DDT and pyrethroids (*11, 28*). The second variant P1842S corresponded to P1874S in *An. gambiae* and P1879 in *M. domestica* and were all in the C-terminal domain (**Table 1**).

154 **Table 1**: Comparative non-synonymous nucleotide variation in the voltage-gated
155 sodium channel gene. The position is relative to the *Anopheles funestus* strain
156 FUMOZ reference, chromosome arm 3RL. Codon numbering according to *Anopheles*
157 *funestus Vgsc* transcript AFUN2_008728.R15290**,** *Anopheles gambiae* transcript
158 AGAP004707-RD in gene set AgamP4.12, and *Musca domestica* EMBL accession
159 X96668 Williamson *et al.* (*29*).

| **Position** | ***An. funestus*** | ***An. gambiae*** | ***M. domestica*** | **Domain** |
|---|---|---|---|---|
| 3RL:44,115,564 T>C | I2030V | I2061 | P2063 | COOH |
| 3RL:44,115,768 C>A | G1962C | A1994 | P1997 | COOH |
| 3RL:44,116,128 G>A | P1842S | P1874S | P1879 | COOH |
| 3RL:44,116,334 T>C | N1773S | N1805 | N1810 | |
| 3RL:44,116,923 A>T | F1638Y | F1670 | V1675 | |
| 3RL:44,117,167 A>T | W1557R | W1589 | W1594 | |
| 3RL:44,122,391 C>A | G1144C | G1173 | G1180 | |
| 3RL:44,125,475 T>A | L976F | L995F | L1014 | IIS6 |

160

161 To explore the possible association between L976F and P1842S alleles with
162 DDT and deltamethrin resistance, we genotyped surviving (resistant) and dead
163 (susceptible) mosquitoes from IR bioassays for both L976Fand P1842S loci). Neither
164 locus was associated with deltamethrin resistance: L976F ($\chi^2$ = 0.04, p = 0.84) and
165 P1842S ($\chi^2$ = 0.59, p = 0.44). (**Fig. 2C**). We found a strong association with DDT
166 resistance in mosquitoes carrying the mutant allele of L976F ($\chi^2$ = 9.23, odds ratio =
167 11.0, p = 0.0024) and a marginally non-significant positive association for P1842S ($\chi^2$
168 = 3.75, p = 0.0528) (**Fig. 2C**).

169 In *An. gambiae*, multiple *kdr* haplotypes have evolved independently (*30, 31*).
170 To elucidate *Vgsc* haplotype structure in *An. funestus,* we computed pairwise linkage
171 disequilibrium (LD) using the Rogers and Huff method (*32*), between
172 nonsynonymous variants occurring at a frequency of > 5% in Tanzanian *An. funestus*
173 **(Fig. 2C**). We found that P1824S occurred in tight LD with L976F (*D'*=0.95) **(Fig. 2D).**

174 Of other non-synonymous polymorphisms, F1638Y and W1557R exhibited only
175 weak LD with L976F (**Fig. 2D)**. We constructed a haplotype clustering dendrogram
176 from haplotypes in all 333 individuals, from the *Vgsc* gene **(Fig. 3).** The clustering
177 dendrogram disclosed three major clades and three main combinations of the four
178 most prevalent *Vgsc* alleles **(Fig. 3).** The most striking signal was a subclade of
179 identical, or near-identical haplotypes containing both L976F and P1842S (**Fig. 3),**
180 indicating a selective sweep on a combined L976F/P1842S haplotype. This combined
181 haplotype was present at higher frequencies in the Morogoro region relative to the
182 neighbouring regions of Pwani, Ruvuma, and Dodoma (**Fig. 3**). Most amino acid
183 substitutions were present in a single clade in samples from Pwani, Dodoma,
184 Ruvuma, and especially Morogoro (**Fig. 3**). This extremely restricted geographic
185 hotspot of *kdr* is in stark contrast to its distribution in *An. gambiae* where *kdr*
186 mutations spread rapidly across vast spatial scales in response to strong selection
187 pressure (*26, 33*).

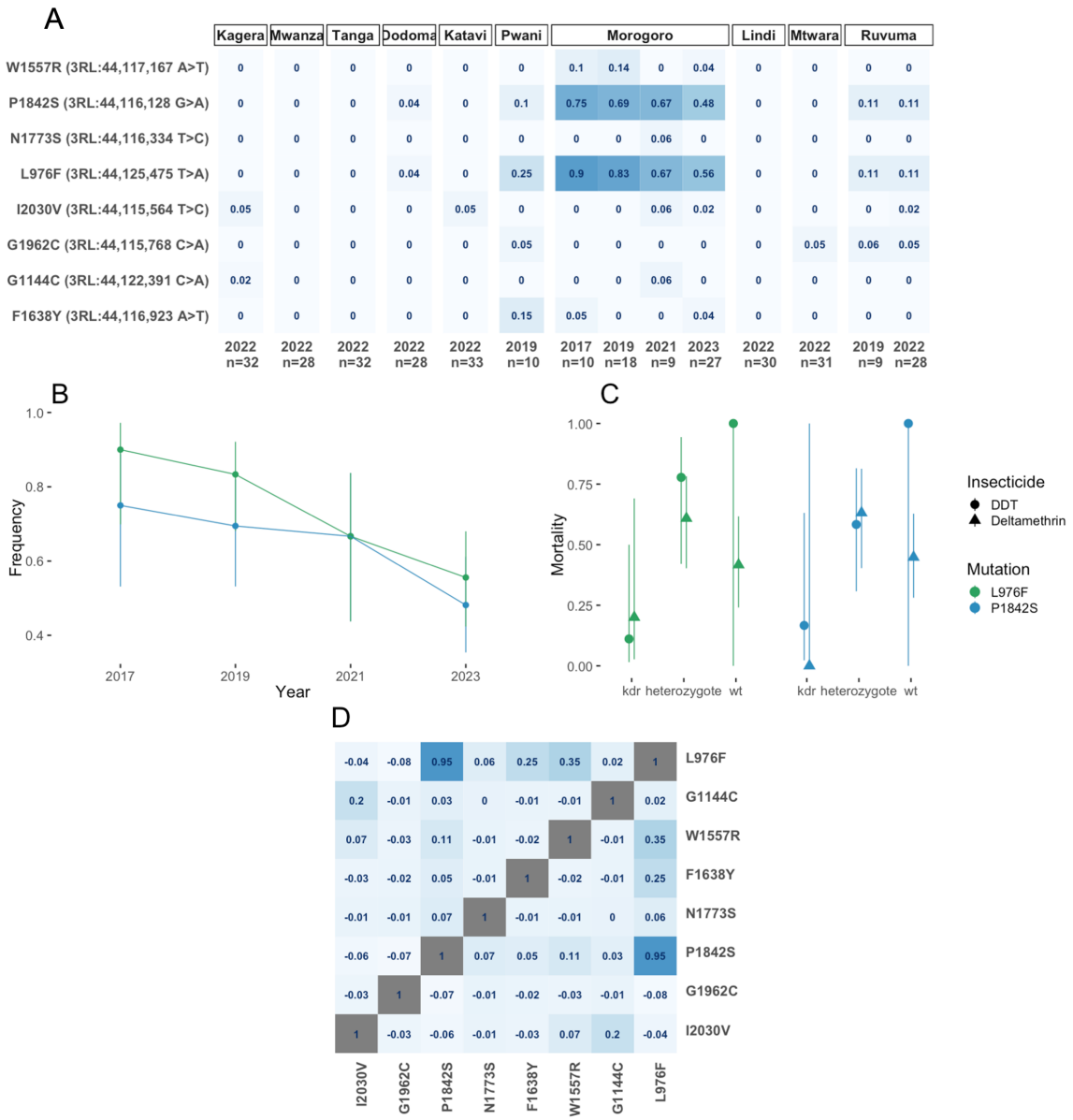


**Fig. 2: (A)** Heatmap of *Vgsc* allele frequencies. Y-axis labels indicate mutation effect, chromosome position, and nucleotide change. X-axis labels indicate the collection date and heatmap intensity indicates frequency where darker = higher, with frequency labelled in each heatmap facet. The heatmap is panelled by the sample collection region. (**B)** L976F and 1842S frequencies, in the Morogoro region, over time. The y-axis indicates allele frequency, X-axis indicates the date. Line and point colour refer to mutation, specified in the legend. Bars indicate 95% confidence intervals. (**C**) Denotes the association of L976F and P1842S with resistance to Deltamethrin and DDT. Colour and panelling are by mutation, the x-axis

198 indicates genotype, the y-axis indicates mortality, the point shape indicates the mean for
199 each insecticide and the line indicates the 95% CI based on generalised mixed model
200 prediction. **(D)** Heatmap of linkage disequilibrium (LD) (Rogers and Huff R) between
201 nonsynonymous variants in the *Vgsc* gene at frequency > 5%. LD is indicated by fill colour.
202 SNP effects and positions are labelled on the X and Y axes.

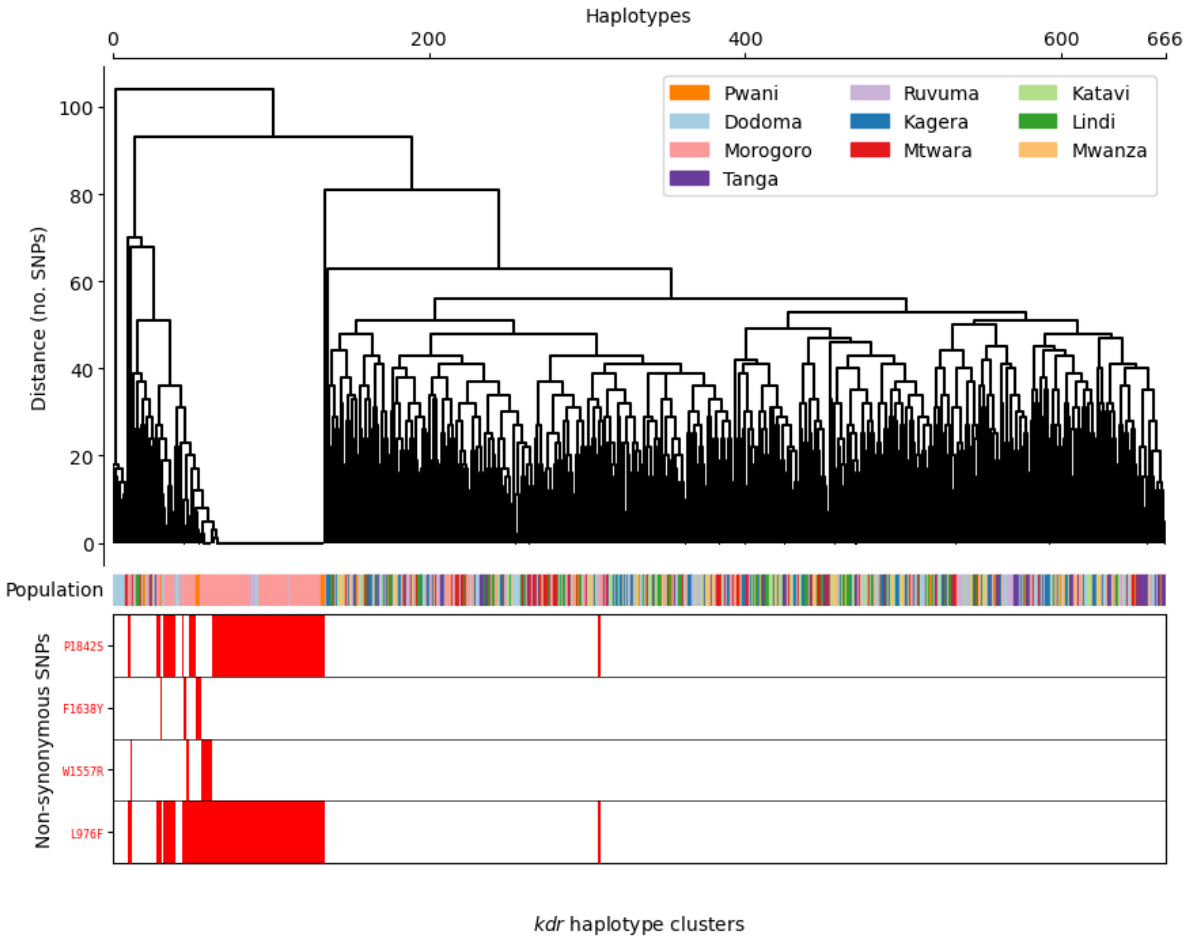


203

204 **Fig. 3:** Clustering of haplotypes at the *Vgsc* gene (LOC125769886, 3RL:44105643-44156624).
205 The dendrogram branch length corresponds to no. SNPs difference (y-axis). Tips correspond
206 to individual haplotypes (x-axis). The coloured Population bar denotes the administrative
207 region of origin (as described by the legend). Red blocks at the bottom indicate the presence
208 of the labelled non-synonymous SNPs in the *Vgsc* gene.

209 DDT is a largely obsolete, banned, pesticide that is no longer widely used for
210 vector control in Tanzania, or in Africa as a whole, due to its bio-accumulative and
211 toxic properties. However, the presence of DDT resistance phenotypes in *An.*

212 *funestus* in Morogoro in 2015 (*34*) suggests *kdr*-mediated resistance to DDT has been
213 present at least since then, and the emergence of *kdr* resistance to DDT suggests that
214 future use of DDT for IRS may become even less favoured. The lack of association of
215 *kdr* with pyrethroid resistance might be due to the strong metabolic resistance shown
216 to pyrethroids in *An. funestus,* reducing the benefit of *kdr* (*35*)**.** However, since our
217 testing included only type II pyrethroids, additional data are required to assess the
218 potential impacts of *kdr* on other pyrethroids and commercial products. The
219 association of *kdr* with resistance to DDT but not pyrethroids, combined with
220 selection signals and recently declining *kdr* allele frequencies where we have time
221 series, suggests recent-past, rather than contemporary selection, perhaps due to
222 factors other than the current use of public health pesticides.

223 **Discussion**

224 In a genomic surveillance study in Tanzanian *An. funestus*, we discovered
225 eight novel *Vgsc* mutations. Two of these, L976F and P1842S, confer *knockdown*
226 *resistance* (*kdr*), occurring in tight linkage disequilibrium and at high frequencies (up
227 to 90%) in the Morogoro region over 4 years, with limited spread to neighbouring
228 regions. The mutation L976F showed an association with resistance to DDT, but not
229 to pyrethroid insecticides. The role of *kdr* in pyrethroid resistance phenotypes in
230 other *Aedes, Culex* and *Anopheles* vectors, makes the discovery of *kdr* in *An. funestus* a
231 significant and unwelcome development that has the potential to pose a new threat
232 to vector control in the region. Reassuringly, a lack of association between *kdr* and
233 deltamethrin resistance indicates that the emergence of *kdr* is not linked to, nor is
234 presently likely to threaten, the mass rollout of PBO-pyrethroid bed nets currently
235 underway in Tanzania as a response to IR(*36*). However, this does not preclude a
236 role for *kdr* in the *An. funestus* IR armamentarium in the future, and an urgent
237 follow-up study is required to determine whether they confer *kdr* resistance
238 phenotypes to other widely used pyrethroids, such as permethrin, and alpha-
239 cypermethrin, as well as other insecticide families, especially PBO and pyrrole

240 formulations currently being rolled out in new ITN products across the African
241 continent (*37*).

242 This discovery raises intriguing questions about the conditions that have
243 enabled the emergence of *kdr* in *An. funestus*. Our data suggests that *Vgsc* mutation in
244 *An. funestus* do not confer target-site resistance to pyrethroids, indicating a possible
245 explanation as to why, despite extreme selection pressures imposed by pyrethroid
246 control have facilitated widespread propagation of resistant *Vgsc* haplotypes across
247 the African continent in *An. gambiae (27)*, the emergence of *kdr* in Tanzanian *An.*
248 *funestus* remains relatively localised. Mechanistic studies, including expression
249 studies of mutant *Vgsc* proteins in *Xenopus* oocytes (*38*)**,** will enable comparisons
250 between taxa that will elucidate this further.

251 If the ubiquitous use of pyrethroids in vector control did not select for the
252 emergence of *kdr*, from whence came *kdr?* Even more curiously, the apparent decline
253 of *kdr* allele frequencies between 2017 and 2023 suggests that the selection pressure
254 causing the emergence of *kdr* has eased (although non-uniform sample sizes per
255 time-point make confident assertion of this difficult). There is no record of DDT use
256 in the last decade for agriculture or vector control in the Morogoro region, or
257 Tanzania as a whole, where the production, importation, and usage of DDT have
258 been banned since 2009 (*17*), except for limited use in malaria vector control. In 2008,
259 Tanzania rolled out an ambitious malaria vector control strategy relying on large-
260 scale use of DDT for indoor residual spraying (IRS), implemented in 60 districts
261 across the country(**Fig. 4A**), and discontinued in 2010 (*39*). Morogoro, where we
262 detected *kdr,* was not part of this expanded campaign. Before the ban, Tanzania
263 imported large stockpiles of DDT mostly for agricultural pest control (**Fig. 4B**).
264 Following the ban, there have been anecdotal reports of continued illegal use of DDT
265 amongst farmers to date (*40*). The Africa Stockpiles Programme (ASP) was launched
266 in 2005 to eliminate stockpiles of obsolete pesticides, including DDT. At this time, it
267 was estimated that Tanzania still possessed approx. 1,500 tonnes of obsolete

pesticides (*41*), including a DDT stockpile of 30 tons (as of 2012) (*42*), approximately 50 km away from where DDT-resistant *An. funestus* were detected in this study, and 156 tons were in Morogoro town (**Fig. 4C**) (*18*). The ASP and the Tanzanian Government eliminated 100% of inventoried publicly held DDT stockpiles and conducted extensive environmental remediation by programme closed in 2013 (*43*). However, extensive DDT contamination remains (*44*), and DDT remains in widespread use by private individuals (*40*). The coincident proximal location of high levels of *kdr* in *An. funestus* with large past DDT stockpiles as well as the presence of widespread DDT contamination and private usage, leads us to hypothesise that the two most likely scenarios of *kdr* emergence in *An. funestus* are contamination of local larval breeding sites from agricultural or stockpiled DDT (**Fig. 4B, C**). The removal of DDT stockpiles by the ASP, and ongoing environmental remediation, may have contributed to reduced selection pressure on *kdr*, evident from declining frequency in Morogoro. Continued monitoring of allele frequencies and future studies of *kdr* frequencies targeted towards sites of known DDT contamination will establish whether this hypothesis is correct.

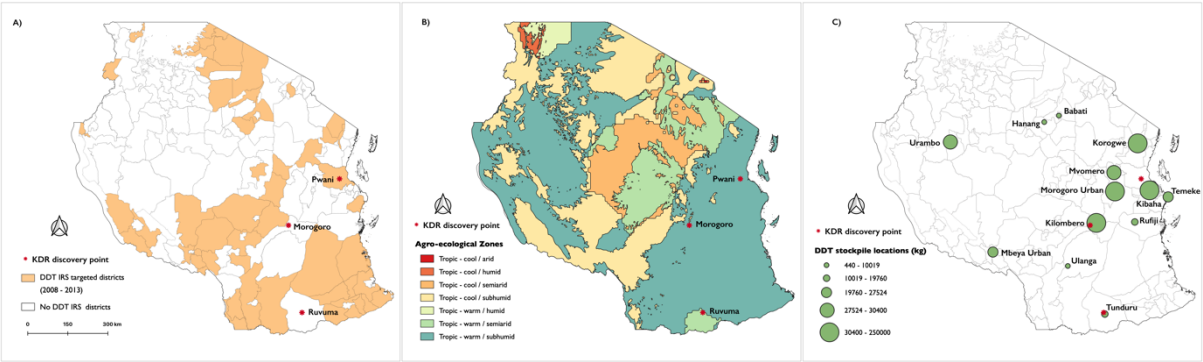


**Fig. 4:** (A) Agro-ecological zones in Tanzania with colours on the map denoting the different categories indicated in the figure key. (B) Tanzanian National Malaria Control Programme (NMCP) indoor residual spraying strategy 2008 – 2012. The colours indicating districts where DDT spraying was planned. (C) DDT stockpile locations with the size of the circle indicating the stockpile quantities.

290 In *Silent Spring* (1962), Rachel Carson brought for the first time into the public
291 eye the unpredictable and often remote impacts of anti-insect chemical agents on
292 human health and nature "On one hand delicate and destructible, on the other
293 miraculously tough and resilient, and capable of striking back in unexpected ways"
294 (*45*). Further study of *kdr* in *An. funestus* will enable the identification of the origin of
295 this mutation and make clear the full implications of its presence in the population
296 for vector control. Whether the emergence of *kdr* in *An. funestus* is caused by vector
297 control, unlicensed DDT usage in agriculture, or exposure to stockpiled DDT, our
298 findings underscore the legacy of *Silent Spring* by reinforcing the potential for
299 pesticides and organic pollutants to exert inadvertent influences on animal biology
300 that may have profound and unfortunate consequences for public health.

301 **Materials and Methods**

302 All scripts and Jupyter Notebooks used to analyse genotype and haplotype data, and
303 produce figures and tables are available from the GitHub repository:
304 https://github.com/tristanpwdennis/kdr_funestus_report_2023

305 **Mosquito collection**

306 *Anopheles funestus* samples analyzed in this study were collected from ten
307 administrative regions in Tanzania: Dodoma, Kagera, Katavi, Lindi, Morogoro,
308 Mtwara, Mwanza, Pwani, Ruvuma, and Tanga (**Figure. 1A**). The collections were
309 done as part of a countrywide *Anopheles funestus* surveillance project in Tanzania
310 and were subsequently incorporated into the MalariaGEN *Anopheles*
311 *funestus* genomic surveillance project database
312 (https://www.malariagen.net/projects/anopheles-funestus-genomic-surveillance-
313 project). Mosquitoes were collected in households between 2017 and 2023 using
314 CDC light traps and mechanical aspirators. They were sorted by sex and taxa and
315 *An. funestus* group mosquitoes preserved individually in 96-well plates containing
316 80% ethanol.

317 **Whole genome sequencing and analysis**

318 The samples were processed as part of the *Anopheles funestus* genomics surveillance
319 MalariaGEN Vector Observatory (VObs) project
320 (https://www.malariagen.net/mosquito).Briefly, the mosquitoes were individually
321 whole-genome-sequenced on an Illumina NovaSeq 6000s instrument. Reads were
322 aligned to the *An. funestus* reference genome AfunGA1 (*46*) with Burrows-Wheeler
323 Aligner (BWA) version v0.7.15. Indel realignment was performed using Genome
324 Analysis Toolkit (GATK) version 3.7-0 RealignerTargetCreator and IndelRealigner.
325 Single nucleotide polymorphisms were called using GATK version 3.7-0
326 UnifiedGenotyper. Genotypes were called for each sample independently, in
327 genotyping mode, given all possible alleles at all genomic sites where the reference
328 base was not "N".

329 Complete specifications of the alignment and genotyping pipelines are available
330 from the malariagen/pipelines GitHub repository
331 (https://github.com/malariagen/pipelines/ ). The aligned sequences in BAM format
332 were stored in the European Nucleotide Archive (ENA).

333 The identification of high-quality SNPs and haplotypes were conducted using BWA
334 version 0.7.15 and GATK version 3.7-0. Quality control involved removal of samples
335 with low mean coverage, removing cross-contaminated samples, running PCA to
336 identify and remove population outliers, and sex confirmation by calling the sex of
337 all samples based on the modal coverage ratio between the X chromosome and the
338 autosomal chromosome arm 3R. Full quality control methods are available on the
339 MalariaGEN vector data user guide (https://malariagen.github.io/vector-
340 data/ag3/methods.html).

341 We used decision-tree filters that identify genomic sites where SNP calling and
342 genotyping is likely to be less reliable. More information on site filters can be found
343 on the MalariaGEN vector data user guide.

344 Genotypes at biallelic SNPs that passed the decision-tree site filtering process were
345 phased into haplotypes using a combination of read-backed and statistical phasing.
346 Read-backed phasing was performed for each sample using WhatsHap version 1.0
347 [https://whatshap.readthedocs.io/]. Statistical phasing was then performed using
348 SHAPEIT4 version 4.2.1 [https://odelaneau.github.io/shapeit4/].

349 Complete specifications of the haplotype phasing pipeline are available from the
350 malariagen/pipelines GitHub repository
351 (https://github.com/malariagen/pipelines/tree/master/pipelines/phasing-vector).

352 **Identification of SNPs on *Vgsc***

353 To identify the *An. funestus Vgsc* gene and the variant that confers target-site
354 resistance we performed alignments between the *An. gambiae* VGSC transcript
355 AGAP004707-RD in AgamP4.12 geneset from the Ag1000 phase 3 data resource
356 (https://www.malariagen.net/data/ag1000g-phase3-snp ) and AFUN2_008728 from
357 the *An. funestus* AfunF1.3 dataset. We extracted single nucleotide polymorphism
358 (SNPs) altering the amino acid of VGSC protein from the *An. funestus* dataset and
359 computed the allele frequency on the mosquito cohorts defined by the region and
360 year of collection ((See **Supp. Table 1** for per region/year sample numbers)). Under
361 selection pressure various alleles are expected to increase in frequency; we therefore
362 filtered out variant alleles with a frequency lower than 5% resulting in a list of 8
363 variant alleles. Multiple sequence alignments of *An. funestus Vgsc* against *An. gambaie*
364 and *M. domestica* were performed using MEGA v11.013.

365 **Population genetic analyses**

366 We searched for signatures of selective sweeps on the *Vgsc* gene using the *G123*
367 selection statistic (*47*)**.** G123 selection scans were performed on *An. funestus*
368 genotypes by collection region where sample *n*>20 **[**see **Figure 1A** and **Supp Table 2]**
369 **]** using the *g123_gwss* function in the malariagen_data python API
370 (https://malariagen.github.io/malariagen-data-python/latest/Af1.html ). Linkage

371 disequilibrium (Rogers and Huff's R-squared) (*32*) between the 8 *Vgsc* alleles was
372 calculated using the *rogers_huff_r_between* in scikit-allel
373 (https://zenodo.org/record/4759368 ). Haplotype clustering was performed by
374 performing hierarchical clustering on a Hamming distance matrix, inferred from
375 phased *An. funestus* haplotypes, using the Scipy library (https://scipy.org/citing-
376 scipy/ ). Clustering dendrogram, and bar plot of amino acid substitutions, was
377 plotted using the seaborn library (*48*).

378

379 **Association of L976F and P1842S alleles with insecticide resistance**

380 To test for associations between the identified mutations with IR, we exposed wild
381 non-blood-fed *An. funestus* mosquitoes of unknown ages to standard doses of
382 deltamethrin and DDT insecticides following the WHO tube assays. For each
383 insecticide, we randomly separated phenotypically resistant mosquitoes (i.e., alive 24
384 hours post-exposure) and susceptible (i.e., dead 24 hours post-exposure) and
385 extracted DNA from individual mosquitoes using DNeasy Blood and Tissue kit
386 (Qiagen, Germany). The mosquitoes were identified at the species level using
387 species-specific primers that can distinguish *An. funestus* from the other members of
388 the group (*49*). To establish if the two *kdr* variants are associated with insecticide
389 resistance, we designed PCR primers from *An. funestus Vgsc* (Gene ID:
390 LOC125769886) to amplify domain IIS6 (L976F) and C-terminal (P1842S) (see **Supp**
391 **Table 3** for primer and thermocycler conditions). The DNA fragments were
392 separated on a 1% agarose gel, cut, purified using PureLink™ Quick Gel Extraction
393 Kit (Invitrogen), and commercially Sanger sequenced. Collectively, we sequenced 76
394 individual mosquitoes: 56 from deltamethrin and the rest from the DDT bioassays.
395 The frequencies of the wild type and mutant alleles were determined and correlated
396 with phenotypes using generalised linear models in R-software v4.1.1.

397 **Data availability**

398 The sequencing data generated in this study have been deposited in the European
399 Nucleotide Archive (https://www.ebi.ac.uk/ena/browser/home ) under study
400 number PRJEB2141.

401

402 **Acknowledgements**

403 This study was supported by funding support was received from the Bill and
404 Melinda Gates Foundation (grant no. INV-002138) to FO, FB, HMF. Howard Hughes
405 Medical Institute-Gates Foundation International Research Scholar Award (grant no.
406 OPP 1099295) to FO, and the Academy Medical Science Springboard Award (ref:
407 SBF007\100094) to FB. The findings and conclusions within this publication are
408 those of the authors and do not necessarily reflect positions or policies of the HHMI,
409 the BMGF or the AMSS.

410 This study was supported by the MalariaGEN Vector Observatory which is an
411 international collaboration working to build capacity for malaria vector genomic
412 research and surveillance and involves contributions by the following institutions
413 and teams. Wellcome Sanger Institute: Lee Hart, Kelly Bennett, Anastasia
414 Hernandez-Koutoucheva, Jon Brenas, Menelaos Ioannidis, Chris Clarkson, Alistair
415 Miles, Julia Jeans, Paballo Chauke, Victoria Simpson, Eleanor Drury, Osama Mayet,
416 Sónia Gonçalves, Katherine Figueroa, Tom Maddison, Kevin Howe, Mara
417 Lawniczak; Liverpool School of Tropical Medicine: Eric Lucas, Sanjay Nagi, Martin
418 Donnelly; Broad Institute of Harvard and MIT: Jessica Way, George Grant; Pan-
419 African Mosquito Control Association: Jane Mwangi, Edward Lukyamuzi, Sonia
420 Barasa, Ibra Lujumba, Elijah Juma. The authors would like to thank the staff of the
421 Wellcome Sanger Genomic Surveillance unit and the Wellcome Sanger Institute
422 Sample Logistics, Sequencing, and Informatics facilities for their contributions.

423 The MalariaGEN Vector Observatory is supported by multiple institutes and
424 funders. The Wellcome Sanger Institute's participation was supported by funding
425 from Wellcome (220540/Z/20/A, 'Wellcome Sanger Institute Quinquennial Review
426 2021-2026') and the Bill & Melinda Gates Foundation (INV-001927). The Liverpool
427 School of Tropical Medicine's participation was supported by the National Institute
428 of Allergy and Infectious Diseases ([NIAID] R01-AI116811), with additional support
429 from the Medical Research Council (MR/P02520X/1). The latter grant is a UK-funded
430 award and is part of the EDCTP2 programme supported by the European Union.

Martin Donnelly is supported by a Royal Society Wolfson Fellowship (RSWF\FT\180003). The Pan-African Mosquito Control Association's participation was funded by the Bill and Melinda Gates Foundation (INV-031595).

The findings and conclusions within this publication are those of the authors and do not necessarily reflect the positions or policies of the funders listed above.

## Contributions

The project was conceived and supervised by FOO, FB, and DW. Field collection was performed by JOO, IHN, HB, and GM. Laboratory analysis, data acquisition and management, and preparing samples for whole genome sequencing were performed by JOO. Sequence QC, alignments, SNP calling, and haplotype phasing were performed by AHK, JN, CSC, and AM. JOO, BP, and TPWD analyzed the data and generated all figures and tables. The manuscript was drafted by JOO and TPWD and revised by all authors. Throughout the project, all authors have contributed key ideas that have shaped the work and the final paper.

## Competing interests

The authors declare no competing interests.

## References

1. S. Bhatt *et al.*, The effect of malaria control on Plasmodium falciparum in Africa between 2000 and 2015. *Nature* **526**, 207- 211 (2015).
2. WHO. (WHO, 2023).
3. P. Berny, Pesticides and the intoxication of wild animals. *J Vet Pharmacol Ther* **30**, 93-100 (2007).
4. C. F. Wurster, Jr., D. H. Wurster, W. N. Strickland, Bird Mortality after Spraying for Dutch Elm Disease with Ddt. *Science* **148**, 90-91 (1965).
5. C. C. Nicholson *et al.*, Pesticide use negatively affects bumble bees across European landscapes. *Nature*, (2023).
6. M. R. Douglas, D. B. Sponsler, E. V. Lonsdorf, C. M. Grozinger, County-level analysis reveals a rapidly shifting landscape of insecticide hazard to honey bees (Apis mellifera) on US farmland. *Sci Rep* **10**, 797 (2020).
7. J. Hemingway, H. Ranson, Insecticide resistance in insect vectors of human disease. *Annu Rev Entomol* **45**, 371-391 (2000).

463 8. T. G. Davies, L. M. Field, P. N. Usherwood, M. S. Williamson, A comparative study of voltage-
464 gated sodium channels in the Insecta: implications for pyrethroid resistance in Anopheline
465 and other Neopteran species. *Insect Mol Biol* **16**, 361-375 (2007).
466 9. J. R. Busvine, Mechanism of resistance to insecticide in houseflies. *Nature* **168**, 193-195
467 (1951).
468 10. L. Grigoraki *et al.*, CRISPR/Cas9 modified An. gambiae carrying kdr mutation L1014F
469 functionally validate its contribution in insecticide resistance and combined effect with
470 metabolic enzymes. *PLoS Genet* **17**, e1009556 (2021).
471 11. L. Reimer *et al.*, Relationship between kdr mutation and resistance to pyrethroid and DDT
472 insecticides in natural populations of Anopheles gambiae. *J Med Entomol* **45**, 260-266
473 (2008).
474 12. J. F. Mosha *et al.*, Effectiveness of long-lasting insecticidal nets with pyriproxyfen-pyrethroid,
475 chlorfenapyr-pyrethroid, or piperonyl butoxide-pyrethroid versus pyrethroid only against
476 malaria in Tanzania: final-year results of a four-arm, single-blind, cluster-randomised trial.
477 *Lancet Infect Dis* **24**, 87-97 (2024).
478 13. M. Accrombessi *et al.*, Efficacy of pyriproxyfen-pyrethroid long-lasting insecticidal nets
479 (LLINs) and chlorfenapyr-pyrethroid LLINs compared with pyrethroid-only LLINs for malaria
480 control in Benin: a cluster-randomised, superiority trial. *Lancet* **401**, 435-446 (2023).
481 14. E. R. Lucas *et al.*, Genome-wide association studies reveal novel loci associated with
482 pyrethroid and organophosphate resistance in Anopheles gambiae and Anopheles coluzzii.
483 *Nat Commun* **14**, 4946 (2023).
484 15. M. J. Donnelly, A. T. Isaacs, D. Weetman, Identification, Validation, and Application of
485 Molecular Diagnostics for Insecticide Resistance in Malaria Vectors. *Trends Parasitol* **32**, 197-
486 206 (2016).
487 16. B. J. Msugupakulya *et al.*, Changes in contributions of different Anopheles vector species to
488 malaria transmission in east and southern Africa from 2000 to 2022. *Parasit Vectors* **16**, 408
489 (2023).
490 17. UNEP. (UNEP, 2005).
491 18. WorldBank. (The World Bank, 2012).
492 19. D. M. Soderlund, D. C. Knipple, The molecular biology of knockdown resistance to pyrethroid
493 insecticides. *Insect Biochem Mol Biol* **33**, 563-577 (2003).
494 20. G. D. Weedall *et al.*, A cytochrome P450 allele confers pyrethroid resistance on a major
495 African malaria vector, reducing insecticide-treated bednet efficacy. *Sci Transl Med* **11**,
496 (2019).
497 21. M. Coetzee, L. L. Koekemoer, Molecular systematics and insecticide resistance in the major
498 African malaria vector Anopheles funestus. *Annu Rev Entomol* **58**, 393-412 (2013).
499 22. J. O. Odero *et al.*, Genetic Markers Associated with the Widespread Insecticide Resistance in
500 Malaria Vector Anopheles funestus Populations across Tanzania. *Research Square* (2024).
501 23. WHO. (WHO, 2023).
502 24. F. D. Rinkevich, Y. Du, K. Dong, Diversity and Convergence of Sodium Channel Mutations
503 Involved in Resistance to Pyrethroids. *Pestic Biochem Physiol* **106**, 93-100 (2013).
504 25. H. Irving, C. S. Wondji, Investigating knockdown resistance (kdr) mechanism against
505 pyrethroids/DDT in the malaria vector Anopheles funestus across Africa. *BMC Genet* **18**, 76
506 (2017).
507 26. P. A. Hancock *et al.*, Modelling spatiotemporal trends in the frequency of genetic mutations
508 conferring insecticide target-site resistance in African mosquito malaria vector species. *BMC*
509 *Biol* **20**, 46 (2022).
510 27. C. S. Clarkson *et al.*, The genetic architecture of target-site resistance to pyrethroid
511 insecticides in the African malaria vectors Anopheles gambiae and Anopheles coluzzii. *Mol*
512 *Ecol* **30**, 5303-5317 (2021).

28. S. N. Mitchell *et al.*, Metabolic and target-site mechanisms combine to confer strong DDT resistance in Anopheles gambiae. *PLoS One* **9**, e92662 (2014).
29. M. S. Williamson, D. Martinez-Torres, C. A. Hick, A. L. Devonshire, Identification of mutations in the housefly para-type sodium channel gene associated with knockdown resistance (kdr) to pyrethroid insecticides. *Mol Gen Genet* **252**, 51-60 (1996).
30. H. Ranson *et al.*, Identification of a point mutation in the voltage-gated sodium channel gene of Kenyan Anopheles gambiae associated with resistance to DDT and pyrethroids. *Insect Mol Biol* **9**, 491-497 (2000).
31. D. Martinez-Torres *et al.*, Molecular characterization of pyrethroid knockdown resistance (kdr) in the major malaria vector Anopheles gambiae s.s. *Insect Mol Biol* **7**, 179-184 (1998).
32. A. R. Rogers, C. Huff, Linkage disequilibrium between loci with unknown phase. *Genetics* **182**, 839-844 (2009).
33. A. Lynd *et al.*, LLIN Evaluation in Uganda Project (LLINEUP) - Plasmodium infection prevalence and genotypic markers of insecticide resistance in Anopheles vectors from 48 districts of Uganda. *medRxiv*, (2023).
34. E. W. Kaindoa *et al.*, Interventions that effectively target Anopheles funestus mosquitoes could significantly improve control of persistent malaria transmission in south-eastern Tanzania. *PLoS One* **12**, e0177807 (2017).
35. G. D. Weedall *et al.*, A cytochrome P450 allele confers pyrethroid resistance on a major African malaria vector, reducing insecticide-treated bednet efficacy. *Sci. Transl. Med*, (2019).
36. Tanzania-NMCP, "Tanzania National Malaria Strategic Plan 2021-2015," (2020).
37. WHO, "Guidelines for malaria - 16 October 2023," (2023).
38. A. J. Miller, J. J. Zhou, Xenopus oocytes as an expression system for plant transporters. *Biochim Biophys Acta* **1465**, 343-358 (2000).
39. R. M. Oxborough, Trends in US President's Malaria Initiative-funded indoor residual spray coverage and insecticide choice in sub-Saharan Africa (2008-2015): urgent need for affordable, long-lasting insecticides. *Malar J* **15**, 146 (2016).
40. J. Lahr, R. Buij, F. Katagira, H. v. d. Valk, "Pesticides in the Southern Agricultural Growth Corridor of Tanzania (SAGCOT) : a scoping study of current and future use, associated risks and identification of actions for risk mitigation," (2016).
41. FAO. (FAO, 2005).
42. UNEP. (2005).
43. WorldBank. (The World Bank, 2016).
44. R. Elibariki, M. M. Maguta, Status of pesticides pollution in Tanzania - A review. *Chemosphere* **178**, 154-164 (2017).
45. R. Carson, *Silent Spring*. (Mariner Books Classics; Anniversary edition, 1962).
46. D. Ayala *et al.*, The genome sequence of the malaria mosquito, Anopheles funestus, Giles, 1900. *Wellcome Open Res* **7**, 287 (2022).
47. A. M. Harris, N. R. Garud, M. DeGiorgio, Detection and Classification of Hard and Soft Sweeps from Unphased Genotypes by Multilocus Genotype Identity. *Genetics* **210**, 1429-1452 (2018).
48. M. L. Waskom, seaborn: statistical data visualization *Journal of Open Source Software* **6**, 3021 (2021).
49. L. L. Koekemoer, L. Kamau, R. H. Hunt, M. Coetzee, A cocktail polymerase chain reaction assay to identify members of the Anopheles funestus (Diptera: Culicidae) group. *Am J Trop Med Hyg* **66**, 804-811 (2002).

562 **Supplementary Table 2**: Samples location and number used in the G123 selection

563 scans. Only locations with n>20

| Admin1_Name | Sample No. |
|---|---|
| Dodoma | 32 |
| Kagera | 32 |
| Katavi | 33 |
| Kigoma | 1 |
| Lindi | 30 |
| Morogoro | 64 |
| Mtwara | 32 |
| Mwanza | 28 |
| Pwani | 12 |
| Ruvuma | 37 |
| Tanga | 33 |

564

565 **Supplementary Table 3**: List of primer sets and cycling conditions used to amplify

566 *Anopheles funestus* VGSC gene

| | | | |
|---|---|---|---|
| kdrL976F_FWD | 5'- TGTGCGGTGAATGGATCGAA-3' | | |
| kdrL976F_REV | 5'-CGCTTCAGCGATCTTGTTGG-3' | | |
| kdrP1842S-FWD | 5'-CTACCCGGGAAATTGTGGCT-3' | | |
| kdrP1842S_REV | 5'-TGCCACCATCGTTTCCGTTA-3' | | |
| | | | |
| Cycling conditions | | | |
| 94 °C | 5min | | |
| 94 °C | 1min | | |
| 58 °C | 30sec | 35 cycles | |
| 72 °C | 30sec | | |
| 72 °C | 10min | | |
| 4 °C | hold | | |

567

568